BJR

Received: 23 June 2015 | Revised: 10 August 2015 | Accepted: 13 August 2015

doi: 10.1259/bjr.20150507

Cite this article as:
Lim C, Malone SC, Avruch L, Breau RH, Flood TA, Lim M, et al. Magnetic resonance for radiotherapy management and treatment planning in prostatic carcinoma. *Br J Radiol* 2015; **88**: 20150507.

PICTORIAL REVIEW

Magnetic resonance for radiotherapy management and treatment planning in prostatic carcinoma

[1]CHRISTOPHER LIM, BM BS, [2]SHAWN C MALONE, MD, [1]LEONARD AVRUCH, MD, [3]RODNEY H BREAU, MD, [4]TREVOR A FLOOD, MD, [5]MEGAN LIM, [3]CHRISTOPHER MORASH, MD, [1]JEFF S QUON, MD, [1]CYNTHIA WALSH, MD and [1]NICOLA SCHIEDA, MD, FRCPC

[1]Department of Medical Imaging The Ottawa Hospital, The University of Ottawa, Ottawa, ON, Canada
[2]Department of Radiation Oncology, The Ottawa Hospital, The University of Ottawa, Ottawa, ON, Canada
[3]Department of Surgery, Division of Urology, The Ottawa Hospital, The University of Ottawa, Ottawa, ON, Canada
[4]Department of Anatomical Pathology, The Ottawa Hospital, The University of Ottawa, Ottawa, ON, Canada
[5]Faculty of Medicine, The University of Saskatchewan, Saskatoon, SK, Canada

Address correspondence to: Dr Nicola Schieda
E-mail: *nschieda@toh.on.ca*

ABSTRACT

MRI has an important role for radiotherapy (RT) treatment planning in prostate cancer (PCa) providing accurate visualization of the dominant intraprostatic lesion (DIL) and locoregional anatomy, assessment of local staging and depiction of implanted devices. MRI enables the radiation oncologist to optimize RT planning by better defining target tumour volumes (thereby increasing local tumour control), as well as decreasing morbidity (by minimizing the dose to adjacent normal structures). Using MRI, radiation oncologists can define the DIL for delivery of boost doses of RT using a variety of techniques including: stereotactic body radiotherapy, intensity-modulated radiotherapy, proton RT or brachytherapy to improve tumour control. Radiologists require a familiarity with the different RT methods used to treat PCa, as well as an understanding of the advantages and disadvantages of the various MR pulse sequences available for RT planning in order to provide an optimal multidisciplinary RT treatment approach to PCa. Understanding the expected post-RT appearance of the prostate and typical characteristics of local tumour recurrence is also important because MRI is rapidly becoming an integral component for diagnosis, image-guided histological sampling and treatment planning in the setting of biochemical failure after RT or surgery.

INTRODUCTION

Prostate cancer (PCa) is the most common non-cutaneous cancer in males[1] with treatment strategies individually tailored according to the risk of biochemical failure (likelihood of recurrence) after locoregional treatment.[2] Curative treatment options include: hormonal treatment, radical prostatectomy (RP) and/or radiotherapy (RT). Active surveillance, the preferred treatment for low-risk/low-volume PCa, is beyond the scope of this article but has been described elsewhere.[3] RT can be used to treat localized or locally advanced PCa and local recurrence following definitive therapy.[4,5] RT aims to eradicate clonogenic tumour cells while minimizing radiation damage to adjacent structures.[4,6] RT can be performed internally (interstitial seed and high-dose rate brachytherapy), externally [conventional, intensity-modulated radiotherapy (IMRT), stereotactic body radiotherapy (SBRT), proton-beam RT] or with combined techniques.[4,6] IMRT has become the standard external RT technique used at most institutions for the management of PCa.[4] IMRT utilizes image guidance, as well as multileaf collimators that move independently in and out of the radiation dose path, creating sharp dose borders confined to the prostate with exceptional sparing of the surrounding organs. Doses delivered by external RT typically range from 75 to 80 Gy.[5] Advantages of RT compared with RP may include lower risks of erectile dysfunction, urinary incontinence, strictures and elimination of the risks associated with surgery.[5] RT toxicities relate to inadvertent injury of adjacent structures including cystitis, urethral strictures and bowel-related complications.[5,7]

With the advent of multiparametric (MP) MRI [T_2 weighted (T2W) + ≥2 functional imaging tests (increasingly diffusion-weighted imaging (DWI) and dynamic contrast enhancement over MR Spectroscopy)], imaging plays an integral role in RT planning. This pictorial review illustrates the utility of MRI in RT for PCa highlighting: locoregional anatomy, pulse sequence selection, RT implant and dominant intraprostatic lesion (DIL) localization and the role of MP-MRI in biochemical recurrence.

Figure 1. 58 year old with Gleason score 4 + 3 = 7 prostate cancer in the right apical peripheral zone (PZ) (not shown) demonstrating the normal prostate and regional pelvic anatomy as depicted with T_2 weighted (T2W) MRI. Axial, coronal and sagittal two-dimensional T2W turbo spin echo (TSE) images demonstrate the normal PZ of increased T2W signal intensity (SI). The PZ is separated from the periprostatic fat by the true capsule, a low T2W SI line (open white arrows in a and b). The neurovascular bundles course lateral to the prostate and are best seen on axial T2W TSE (white arrows in a). The prostate is separated from the rectum (R) by the low T2W SI Denonvillier's fascia (dotted arrows in a and c). The seminal vesicles are appreciated (asterisks in b and c) separate from the rectum and sigmoid colon (SC). Also note the urethra (black arrows in a and c) and the urinary bladder (UB).

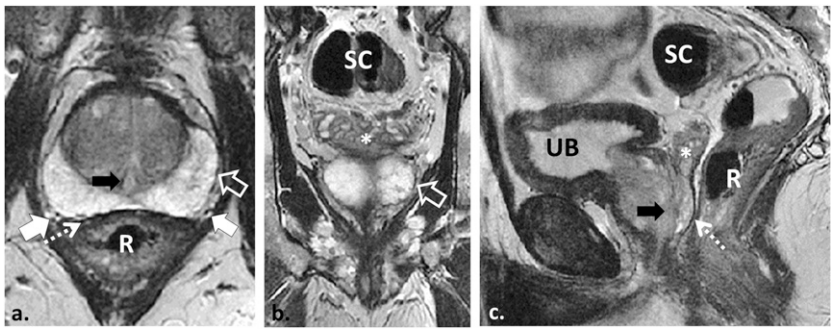

MR Assessment of regional anatomy, local staging and dominant tumour detection

Regional anatomy

The anatomy of the prostate/adjacent structures is best evaluated with T2W turbo/fast spin echo (TSE/FSE) (Figure 1). Conventional 2-dimensional or 3-dimensional TSE/FSE can be used (Figure 2; Table 1). The prostate gland is divided into (a) peripheral zone; harbouring 70% of cancers,[4] (b) transition zone (TZ) and (c) central zone (CZ) (Figure 1). The CZ/TZ are often collectively referred to as the "central gland" (although the CZ can frequently be distinguished seperated from the TZ at the prostate base) which contain 30% of PCa, which are increasingly recognized as clinically important.[4] The apex and base of the prostate are difficult to delineate accurately on CT and MRI better defines the margins of the prostate, which is critical for RT contouring.[8] The bowel, urinary bladder and urogenital diaphragm are also important structures to delineate during RT planning to minimize morbidity (Figures 1–3).

Local staging

MP-MRI is the reference standard imaging test for local staging of PCa.[2,4,5] MRI has a recognized role in staging of

Figure 2. 61 year old undergoing radiotherapy (RT) planning MRI for stereotactic body radiotherapy. Axial (a) and sagittal (b) two-dimensional (2D) T_2 weighted (T2W) fast spin echo (FSE) images depict the prostate and locoregional anatomy. Each high-resolution T2W FSE sequence requires approximately 5 mins to complete, for a total of 15 mins of scan time due to three plane acquisition. Axial (c) and sagittal (d) reconstructed images from source coronal 3-dimensional (3D) FSE (not shown) illustrate how 3D FSE can replace multiplanar 2D FSE for time savings in RT planning. The 3D FSE sequence was acquired in 7 mins, and axial/sagittal reconstructions were performed after the examination was completed; however, there is a decrease in resolution with 3D compared with 2D techniques.

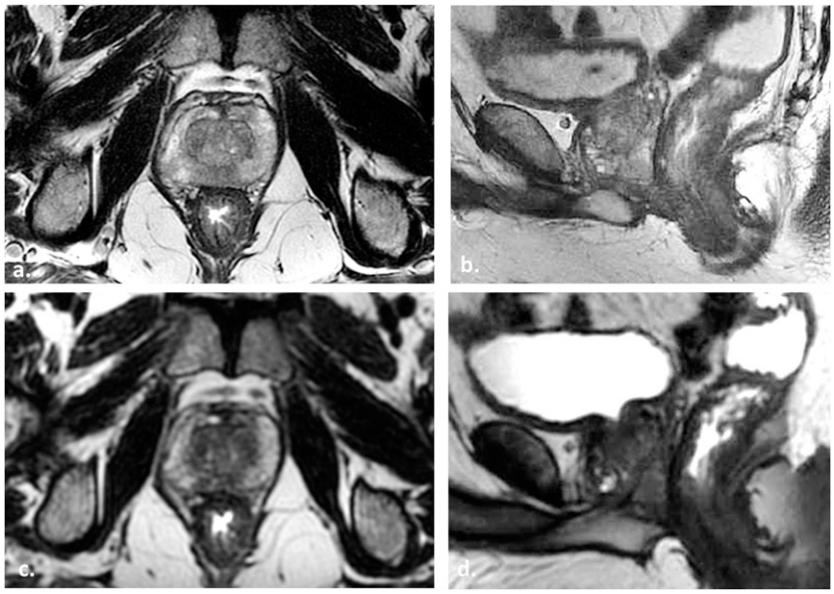

Table 1. Advantages and disadvantages of available pulse sequences for radiotherapy treatment planning examinations with MRI

Pulse sequence	Advantages	Disadvantages
T2W two-dimensional fast/turbo spin echo	Best depiction of the prostate gland zonal anatomy and regional anatomy	Time consuming to perform in three planes
	Robust, high spatial resolution, low blur	Poor depiction of fiducials
T2W three-dimensional fast/turbo spin echo	Can be reconstructed in any imaging plane, potentially saving time	Long acquisition times
	Increased SNR	Vulnerable to motion degradation
	Thin (<1 mm) source slice thickness	Images degraded by blur owing to extended echo train
		Poor depiction of fiducials
T1W single-echo (spoiled) GRE	Fast acquisition times (breath-hold)	Poor spatial resolution (although can be increased) at the cost of increased imaging time
	Better depiction of fiducials when compared with spin echo	Limited contrast resolution, limited depiction of anatomy
		Geometric distortion and warping effects from implanted fiducials
Multiecho GRE	Increased SNR and improved resolution compared with single-echo gradient echo	Time consuming (4–5 mins)
	Optimal depiction of fiducials and other implanted devices	Vulnerable to motion degradation
	T_2* weighted image—provides better contrast resolution than single-echo GRE	
Diffusion-weighted imaging	Depicts dominant tumour foci in the PZ and TZ with high sensitivity	Time consuming (5 mins)
	Quantitative ADC correlates with Gleason score of tumour	Image quality degraded by implanted fiducials/ seeds and post-RP surgical clips
T1W dynamic contrast enhancement	Can be used to confirm PZ tumour foci in combination with diffusion-weighted imaging	Requires gadolinium
	Less susceptible to artefact from fiducials/seeds and post-RP surgical clips compared with diffusion-weighted imaging	Overlap in imaging features between benign prostatic hyperplasia and tumours in the TZ
	Limited for the evaluation of the TZ	

GRE, gradient recalled echo; PZ, peripheral zone; RP, radical prostatectomy; SNR, signal-to-noise ratio; T1W, T_1 weighted; T2W, T_2 weighted; TZ, transition zone.

intermediate/high-risk PCa.[2] Reported accuracies of MRI for assessment of extraprostatic extension (EPE) and seminal vesicle invasion (SVI) varies,[9] with a previous meta-analysis showing pooled sensitivity and specificity of 71% and 82%, respectively.[9] Accurate local staging is critical for determining the optimal treatment strategy and impacts RT planning. If

Figure 3. Depiction of the urogenital diaphragm at 3.0-T MRI. Coronal and sagittal T_2 weighted (T2W) turbo spin echo (TSE) images in three different patients imaged with two-dimensional T2W TSE using endorectal coil (a), surface coil (b) and three-dimensional TSE with surface coil (c) illustrate the normal genitourinary (GU) diaphragm (white arrows, open black arrows and dotted arrows, respectively). The GU diaphragm which is defined as the two layers of fascia enclosing the deep transverse perineal muscle and the external sphincter of the urethra is readily depicted on T2W MRI as a flat plate of fibromuscular tissue suspended between the inferior pubic rami just below the pubic symphysis. The GU diaphragm is an important structure to identify in radiotherapy treatment planning because it helps to define the prostate apex which is difficult to visualize with CT simulation scans.

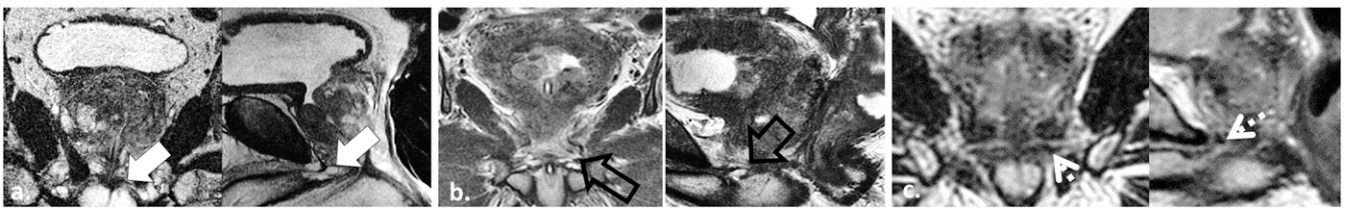

Figure 4. 55 year old undergoing radiotherapy planning multiparametric (MP)-MRI for stereotactic body radiotherapy. Axial T_2 weighted (T2W) fast spin echo (a), axial apparent diffusion coefficient map (b) and axial image obtained from dynamic contrast-enhanced sequence (c) demonstrate a low T2W signal intensity lesion in the left mid-peripheral zone (white arrow in a) with mild restricted diffusion (white arrow in b) and a Type III washout curve (c) consistent with patient's known tumour in this location. Axial multiecho gradient recalled echo image (d) depicts two platinum fiducial markers (dotted arrows) which enable the treatment planning MP-MRI to be fused onto treatment planning CT images (not shown).

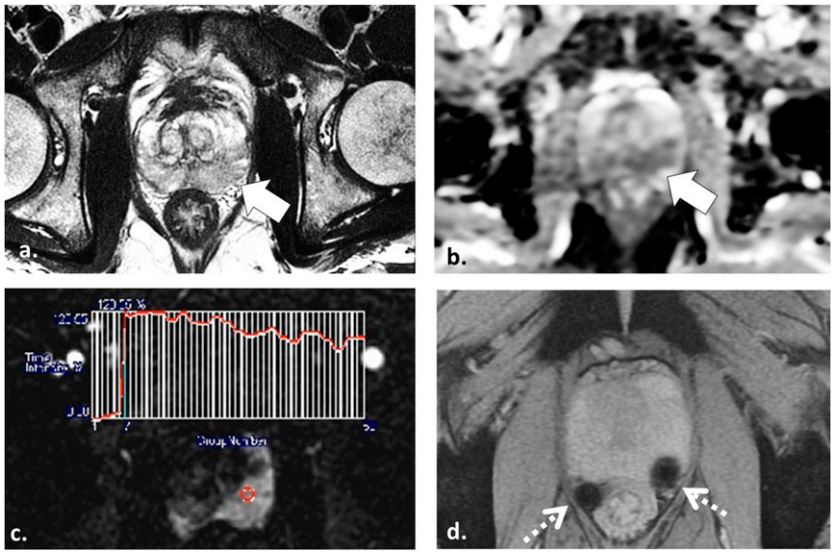

EPE or SVI is detected, patients are not suitable candidates for brachytherapy alone.[2,4,5] With SVI, seminal vesicles are treated to full dose. Without SVI, seminal vesicles may be included within the target volume with RT tailored to a dose sufficient to treat microscopic disease, thereby decreasing morbidity.[10]

Dominant intraprostatic tumour lesion detection

MP-MRI is highly accurate for detecting clinically significant (Gleason score $\geq 3+4=7$) PCa[1] (Figures 4 and 5). Biochemical failure from locally recurrent tumour after RT is usually at the site of the DIL.[4,7] Boosting the DIL with RT can

Figure 5. 57 year old undergoing radiotherapy planning multiparametric MRI for stereotactic body radiotherapy. Axial two-dimensional (a) and three-dimensional (3D) (b) T_2 weighted (T2W) fast spin echo, axial apparent diffusion coefficient (ADC) map (c) and axial image obtained from dynamic contrast-enhanced (DCE) sequence (d) demonstrate a low T2W signal intensity lesion in the left mid-peripheral zone (white arrows in a and b) with corresponding mild restricted diffusion (white arrow in c) and a Type II contrast curve with steep upslope of enhancement (d) in keeping with the patient's known Gleason score $3+3=6$ tumour in this location. Axial multiecho gradient recalled echo (ME-GRE) images (e) depict a fiducial marker at the right prostatic capsule at the same level of the tumour (dotted arrow). Fusion of the T2W, ADC or in this case DCE data onto the ME-GRE images (f) enables accurate three-dimensional localization of the tumour (open white arrow) with respect to the implanted fiducials (arrowhead).

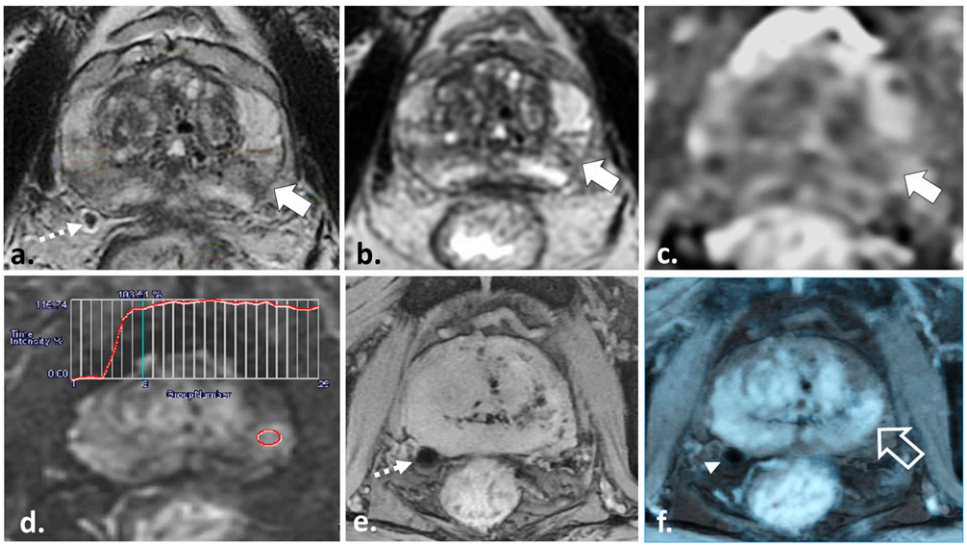

Figure 6. 52 year old with Gleason score 3 + 4 = 7 tumour who underwent pre- and post-brachytherapy MRI (for local staging and post-brachytherapy treatment planning, respectively) demonstrates the challenge of tumour detection after implant insertion. Axial T_2 weighted (T2W) fast spin echo (a), axial apparent diffusion coefficient map (b) and axial image obtained from dynamic contrast-enhanced sequence (c) demonstrate a low T2W signal intensity focus in the left apical peripheral zone (white arrow in a) with corresponding restricted diffusion (white arrow in b) and focal hyperenhancement (white arrow in c) in keeping with the patient's known tumour in this location. Post-implant axial T2W turbo spin echo (e) and axial multiecho gradient recalled echo image (f) depicts multiple brachytherapy seeds which were inserted in the interim adequately covering the prostate gland and dominant tumour. Localization of the dominant tumour focus with MRI is nearly impossible after brachytherapy seed insertion; however, in this case, it can be inferred from pre-treatment MRI and is depicted by the dotted white arrows in (e) and (f).

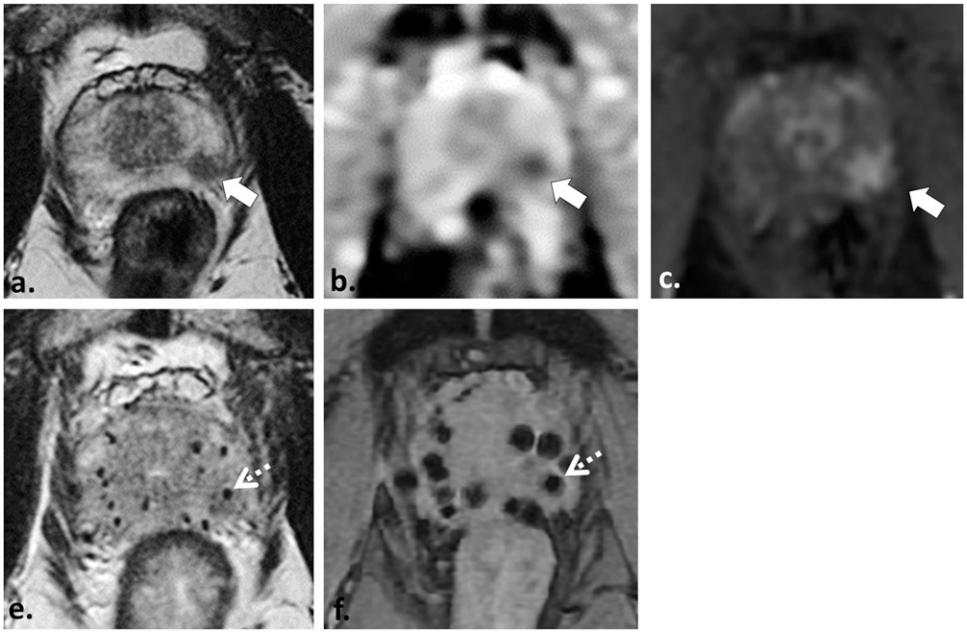

be performed accurately with image-guided radiotherapy (IGRT) techniques (Figure 5). With external IGRT, implanted fiducials or tracking systems are used to co-register data from MP-MRI to treatment planning systems. Localization of DILs and staging with MP-MRI should be performed before fiducial markers or interstitial seeds are placed because the implanted devices and/or post-implant procedural changes may compromise interpretation and cause errors (Figures 6 and 7).

Implanted fiducials and brachytherapy seeds

Implanted devices are placed for direct treatment (brachytherapy seeds) or for IGRT (fiducial markers).[4] Interstitial brachytherapy places radioactive seeds either on a temporary (high-radiation

Figure 7. 60 year old with Gleason score 3 + 3 = 6 tumour in the right apical peripheral zone (PZ) underwent MRI for radiotherapy planning of stereotactic body radiotherapy. Axial T_2 weighted (T2W) fast spin echo image (a) demonstrates two implanted platinum fiducial markers (dotted white arrows) and a low T2W signal intensity (SI) region in the left mid-PZ (white arrow). This area was reported as suspicious for tumour and extraprostatic extension. Corresponding axial T_1 weighted (T1W) gradient recalled echo image (b) demonstrates the implanted fiducials (dotted white arrows) and that the area detected on T2W shows increased T1W SI (open white arrow) consistent with post-procedural haemorrhage. Axial trace b1000 $mm^2 s^{-1}$ echo-planar image (c) is limited by distortion artefact from the implanted fiducials (white arrows). Dynamic contrast-enhanced data (not shown) were similarly limited by artefact from fiducials.

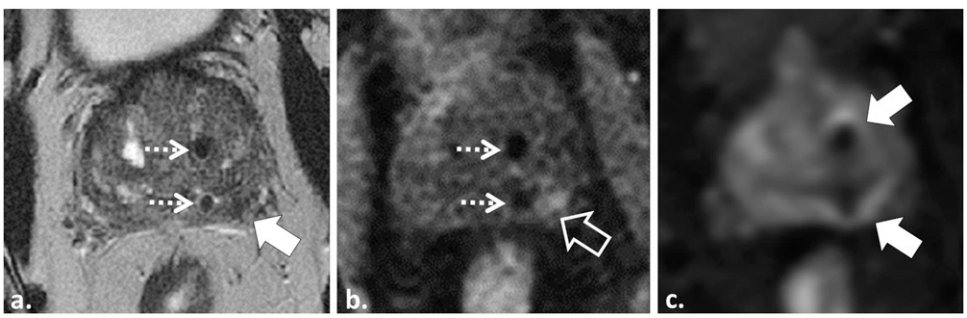

Figure 8. 57 year old undergoing radiotherapy (RT) planning MRI for intensity-modulated radiotherapy after insertion of three gold seed fiducial markers. Axial T_1 weighted (T1W) in-phase (IP) gradient recalled echo (GRE) image (a) barely demonstrates the gold fiducial marker (white arrow). Axial multiecho gradient recalled echo (ME-GRE) image (b) provides better depiction of the gold fiducial marker (open white arrow). A 52-year-old patient undergoing RT planning MRI for stereotactic body radiotherapy after insertion of three platinum fiducial markers demonstrates improved visualization of platinum compared with gold fiducials owing to the greater magnetic susceptibility of platinum. The platinum fiducial (solid white arrows) is easily identified on both T1W IP GRE (c) and ME-GRE (d).

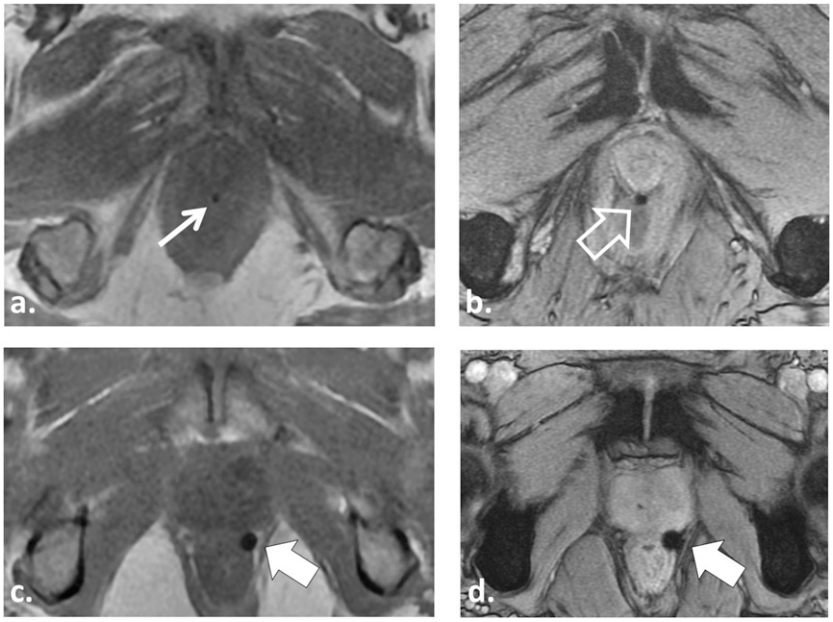

dose rate) or permanent (low-radiation dose rate) basis[4] typically using a transperineal approach with trans-rectal ultrasound (TRUS) guidance.[3] At our institution, iodine-125 seeds encased in titanium containing silver markers (I-125 Rapid Strand™, GE Healthcare, Mississauga, ON) are used delivering approximately 145 Gy (Figure 8). Fiducial markers are used for IGRT to track the prostate and facilitate co-registration of MP-MR data during RT planning.[4,11] Fiducial markers are used to compensate for mis-registration between the expected and actual location of the target that occurs owing to both intrafractional and interfractional motion.[4,11] Motion may be related to patient positioning, adjacent bladder and bowel position/capacity, and treatment-related prostate volume changes.[7] Markers are typically inserted using a transrectal approach with TRUS guidance.

Implanted fiducials and brachytherapy seed migration are common, occurring in up to 25% of patients.[7] It is important to include large field-of-view images of the pelvis to assess for displaced seeds/fiducials. In the case of brachytherapy seed migration, this may result in inaccurate dosimetry, treatment planning errors and possible morbidity to distal organs.[7] To minimize tracking errors for IGRT, at our institution, we allow a minimum 7–10 days after implantation before imaging to ensure the fiducials undergo fibrosis and are more permanently fixed within the prostate. Despite the popularity of gold markers, at our institution, we currently use platinum fiducials. Platinum fiducials have improved depiction on MRI (owing to higher magnetic susceptibility), similar visualization on radiography/CT and similar safety profiles compared with gold fiducials (Figures 4 and 8).[11]

Figure 9. 64 year old undergoing radiotherapy planning MRI after placement of interstitial brachytherapy seeds. Axial T_2 weighted fast spin echo image (a) barely depicts the implanted seeds. Axial T_1 weighted in-phase gradient recalled echo (GRE) image (b) demonstrates the seeds, but image quality is degraded by spatial distortion and image blur. Axial multiecho GRE image (c) provides the best depiction of the implanted seeds.

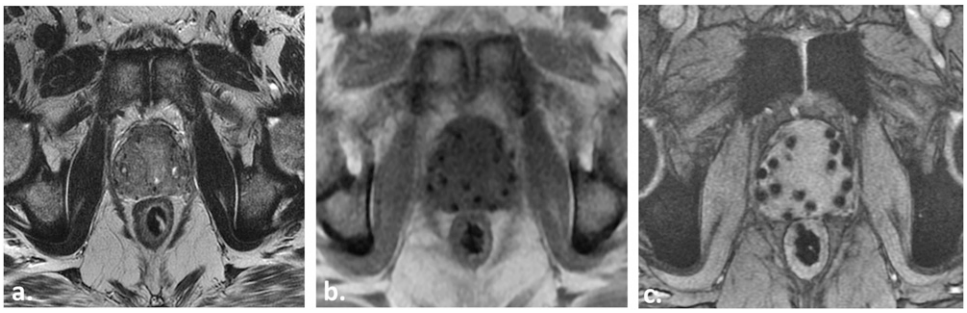

Table 2. Sequence parameters for radiotherapy planning MRI of the prostate performed with pelvic surface coil[a] at 3.0 T[b]

Available pulse sequences	Imaging Plane	Field of view (mm)	Matrix size (mm)	Slice thickness/ gap (mm)	Repetition time/TE (ms)	Echo train length	Flip angle (degrees)	Acceleration factor	Receiver bandwidth (Hz/voxel)	Acquisition time (min)	Number of signals averaged
Anatomic pulse sequences											
T_2 2D TSE[c]	Axial	220 × 220	320 × 256	2–3.0/0	3890–5250/ 105–125	27–35	111	N/A	122	4 min	1–2
T2 3D TSE/FSE[d]	Axial[e]	350 × 350	352 × 352	0.8–2.4[e]	2000/80	120	111	2	100	5–7	1–2
Sequences for detection of implanted device											
T_1 3D dual-echo GRE	Axial	240 × 240	292 × 224	4.0/1.0	4.8/TE1: 1.1–1.3; TE1: 2.2–2.5	NA	12	2	558	Breath-hold	1
Multiecho GRE[f]	Axial	400	288 × 288	1.4/0	2000/60–121	120	110	2	91	4 : 25	2
Functional (parametric) pulse sequences											
Diffusion-weighted imaging[g]	Axial	280 × 280	128 × 80	3–4.0/0	4200/90	1	90	2	1950	5 min	4–10
T_1 GRE dynamic contrast[h]	Axial	220 × 220	128 × 128	4.0/0	NA	NA	12	2	488	6 min	1

2D, two-dimensional; 3D, three-dimensional; GRE, gradient recalled echo; NA, not applicable; TSE, turbo echo spin.
[a]Integrated pelvic surface coils (4–16 channels) with activated spine coils (8–12 channels).
[b]Clinical 3.0-T systems: TRIO TIM (Siemens Healthcare, Malvern, PA) and Discovery 750 W (GE Healthcare, Milwaukee, WI).
[c]2D turbo/fast spin echo.
[d]3D turbo/fast spin echo (SPACE, Siemens Medical; CUBE, GE Healthcare).
[e]Source data is acquired in the axial plane at 0.8-mm intervals and reconstructed in the coronal and sagittal plane at 2.0-mm intervals.
[f]Multiecho GRE (MEDIC, Siemens Healthcare; MERGE, GE Healthcare).
[g]DWI performed with spectral fat suppression echoplanar imaging with tri-directional motion probing gradients and *b* values of 0, 500, 1000 with automatic apparent diffusion coefficient (ADC) map generation.
[h]Dynamic fast spoiled 2D GRE performed with a temporal resolution of 10 s after injection of 0.2 mmol kg^{-1} of gadobutrol (Gadovist, Bayer Inc., Toronto, ON) at a rate of 3 ml s^{-1}.

Figure 10. 76 year old undergoing multiparametric MRI after external beam radiotherapy (RT) owing to biochemical failure to assess for locally recurrent tumour. Axial T_2 weighted (T2W) fast spin echo (FSE) images (a–c) demonstrate the post-RT prostate and seminal vesicles. The seminal vesicles are of low T2W signal intensity (SI) and are atrophic (black arrows). The prostate has atrophied, is of low T2W SI, and the delineation of the normal prostatic anatomy is obscured (white arrows). At the level of the prostate apex, axial T2W FSE (d), axial apparent diffusion coefficient map (e) and axial image obtained from dynamic contrast-enhanced sequence (f) demonstrate a focal low T2W SI nodule (black arrow in d) with restricted diffusion (white arrow in e) and a Type II contrast curve with rapid onset and steep upslope of enhancement in (f). The tumour at initial trans-rectal ultrasound (TRUS) biopsy pre-RT was in the left apical region. The diagnosis of locally recurrent tumour was subsequently confirmed with targeted TRUS biopsy.

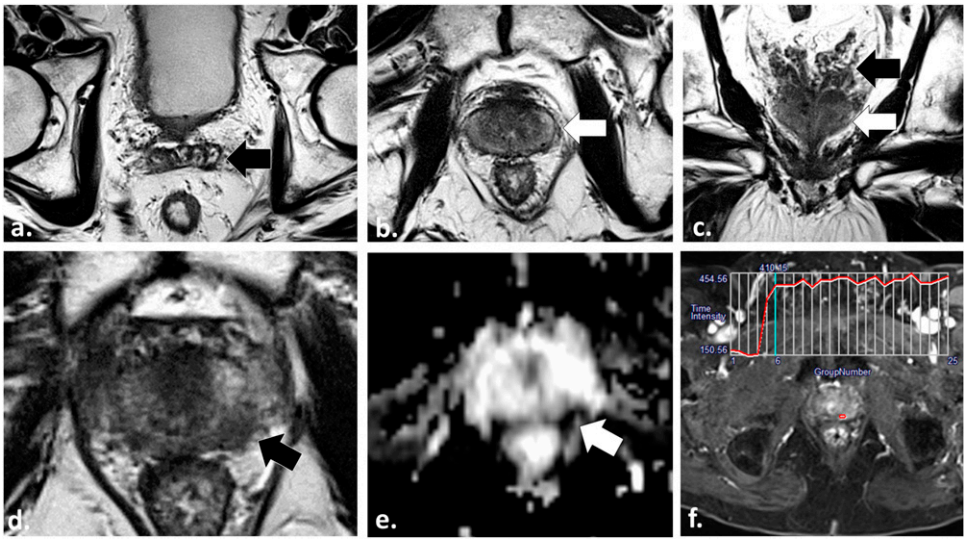

MRI localization of implanted devices

Depiction of implanted devices with MRI is important.[11] Detection with MRI relies on the local T_2^* effects induced by the implants. In general, gradient recalled echo (GRE) sequences provide better depiction of implants owing to the lack of a 180° refocusing pulse that is associated with TSE/FSE (Table 1; Figure 8). Recently, the use of multiecho combined GRE has been described as an alternative sequence providing optimal depiction of implants while maintaining image quality and sharpness (Figure 9; Table 2).[11]

Multiparametric MRI in biochemical failure

The post-radiotherapy prostate gland

Expected morphological changes occur in the prostate and seminal vesicles after RT (Figure 10) including atrophy which may obscure the normal zonal anatomy resulting in diffuse low T2W signal[7,12] and reduced apparent diffusion coefficient values on DWI due to chronic inflammation/fibrosis.[7,12]

Biochemical failure: evaluation of locally recurrent tumour

Biochemical failure is defined according to the American Society for Radiation Oncology (ASTRO)–Phoenix criteria of a nadir PSA level + 2 ng ml^{-1}.[12] Biochemical failure may be due to systemic disease or local recurrence.[7,12] The use of ^{11}C-choline positron emission tomography (PET)-CT or PET-MRI can be highly accurate in the setting of biochemical failure (Figure 11); however, its role is currently incompletely defined, and accessibility is a limitation in many centres.[7,12] MP-MRI, compared with T2W imaging alone, is more accurate for detection of locally recurrent tumour (Figure 10).[12] Following RT, local recurrence most commonly occurs at the site of the original DIL, which should be scrutinized carefully on follow-up imaging, Figure 10.[7,12] Following RP, recurrent tumour is most commonly seen at the vesicourethral anastomosis, seminal vesicle bed or along the posterior bladder and anterior rectal walls.[4,12] Lesions detected at MP-MRI can be targeted with TRUS guidance improving the yield of histological confirmation (Figure 11).[12,13]

Following RT, when the diagnosis of locally recurrent tumour is established, the various salvage therapy techniques include RP, cryoablation, high-intensity focused ultrasound (HIFU) and RT.[14] Salvage RT is the first-line treatment in the absence of systemic disease and offers a potential chance of cure. If systemic disease is present, androgen deprivation is preferred.[5,7] MRI plays an important role in RT planning, enabling accurate target definition. Areas of disease on MRI can be boosted using IGRT to optimize local tumour control and further to minimize dose to potentially previously irradiated adjacent pelvic structures. RP provides a form of radical treatment; however, salvage RP following RT is technically challenging with higher risks of post-surgical complications owing to the post-RT related changes in the pelvis and obliteration of normal tissue planes.[14] Newer focal therapies for salvage include cryoablation and HIFU techniques, which show promise with lower side effect profiles; however, efficacy and long-term outcomes are lacking.[14]

In conclusion, MP-MRI of the prostate is important for RT planning providing accurate depiction of locoregional

Figure 11. A 52-year-old male with locally recurrent tumour in the left seminal vesicle after radical prostatectomy. Axial T_2 weighted (T2W) fast spin echo image (a) shows a non-specific intermediate T2W signal intensity nodule lateral to the left seminal vesicle (white arrow) adjacent to surgical clips (arrowhead). Axial echoplanar image and axial apparent diffusion coefficient map (b, c) are non-diagnostic owing to severe warping and geometric distortion (open arrows). Axial post-gadolinium enhanced T_2 weighted image (d) shows the nodule is enhancing (white arrow) but dynamic contrast-enhanced analyses were corrupted by motion and artefact related to the surgical clips (arrowhead). The study was interpreted as suspicious but indeterminate. ^{11}C-choline positron emission tomography was performed (e) showing uptake in the nodule (arrows) adjacent to surgical clips (arrowhead). CT-targeted biopsy was attempted (f) which was non-diagnostic, and ultimately a MR-TRUS fusion biopsy was performed (g) illustrating the nodule surrounded by surgical clips (arrowheads). Histopathology results confirmed Gleason score 4 + 5 = 9 prostate cancer.

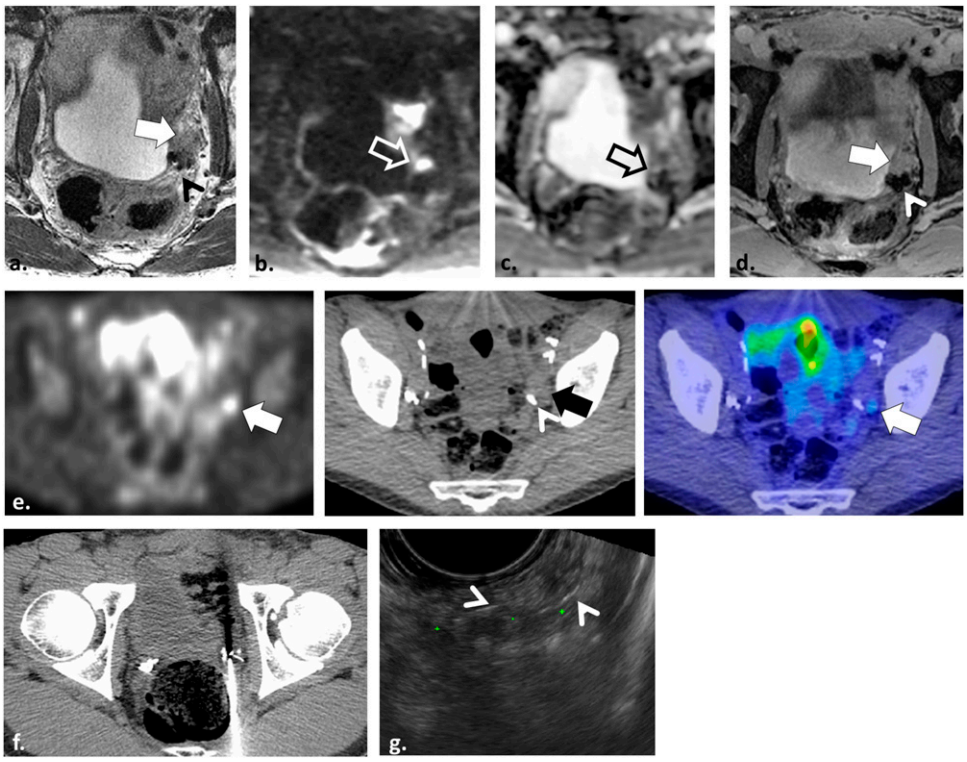

anatomy and DIL, local staging and depiction of implanted devices. MP-MRI can be used to optimize RT planning for boosting the DIL and to minimize dose to adjacent structures. Through MP-MRI, locally recurrent tumour can be accurately identified in the setting of biochemical recurrence and can be used to improve histological confirmation through targeted biopsy and optimize treatment planning when salvage RT is prescribed.

REFERENCES

1. de Rooij M, Hamoen EH, Futterer JJ, Barentsz JO, Rovers MM. Accuracy of multiparametric MRI for prostate cancer detection: a meta-analysis. *AJR Am J Roentgenol* 2014; **202**: 343–51. doi: 10.2214/AJR.13.11046
2. Barentsz JO, Richenberg J, Clements R, Choyke P, Verma S, Villeirs G, et al; European Society of Urogenital Radiology. ESUR prostate MR guidelines 2012. *Eur Radiol* 2012; **22**: 746–57. doi: 10.1007/s00330-011-2377-y
3. Fascelli M, George AK, Frye T, Turkbey B, Choyke PL, Pinto PA. The role of MRI in active surveillance for prostate cancer. *Curr Urol Rep* 2015; **16**: 42. doi: 10.1007/s11934-015-0507-9
4. Boonsirikamchai P, Choi S, Frank SJ, Ma J, Elsayes KM, Kaur H, et al. MR imaging of prostate cancer in radiation oncology: what radiologists need to know. *Radiographics* 2013; **33**: 741–61. doi: 10.1148/rg.333125041
5. Mohler J, Bahnson RR, Boston B, Busby JE, D'Amico A, Eastham JA, et al. NCCN clinical practice guidelines in oncology: prostate cancer. *J Natl Compr Canc Netw* 2010; **8**: 162–200.
6. Das S, Liu T, Jani AB, Rossi P, Shelton J, Shi Z, et al. Comparison of image-guided radiotherapy technologies for prostate cancer. *Am J Clin Oncol* 2014; **37**: 616–23. doi: 10.1097/COC.0b013e31827e4eb9
7. Schieda N, Malone SC, Al Dandan O, Ramchandani P, Siegelman ES. Multimodality organ-based approach to expected imaging findings, complications and recurrent tumour in the genitourinary tract after radiotherapy. *Insights Imaging* 2014; **5**: 25–40. doi: 10.1007/s13244-013-0295-z
8. Tanaka H, Hayashi S, Ohtakara K, Hoshi H, Iida T. Usefulness of CT-MRI fusion in radiotherapy planning for localized prostate

cancer. *J Radiat Res* 2011; **52**: 782–8. doi: 10.1269/jrr.11053

9. Engelbrecht MR, Jager GJ, Laheij RJ, Verbeek AL, van Lier HJ, Barentsz JO. Local staging of prostate cancer using magnetic resonance imaging: a meta-analysis. *Eur Radiol* 2002; **12**: 2294–302. doi: 10.1007/s00330-002-1389-z
10. Bayman NA, Wylie JP. When should the seminal vesicles be included in the target volume in prostate radiotherapy? *Clin Oncol (R Coll Radiol)* 2007; **19**: 302–7. doi: 10.1016/j.clon.2007.03.005
11. Schieda N, Avruch L, Shabana WM, Malone SC. Multi-echo gradient recalled echo imaging of the pelvis for improved depiction of brachytherapy seeds and fiducial markers facilitating radiotherapy planning and treatment of prostatic carcinoma. *J Magn Reson Imaging* 2015; **41**: 715–20. doi: 10.1002/jmri.24590
12. Barchetti F, Panebianco V. Multiparametric MRI for recurrent prostate cancer post radical prostatectomy and postradiation therapy. *Biomed Res Int* 2014; **2014**: 316272. doi: 10.1155/2014/316272
13. Menard C, Iupati D, Publicover J, Lee J, Abed J, O'Leary G, et al. MR-guided prostate biopsy for planning of focal salvage after radiation therapy. *Radiology* 2015; **274**: 181–91. doi: 10.1148/radiol.14122681
14. Kimura M, Mouraviev V, Tsivian M, Mayes JM, Satoh T, Polascik TJ. Current salvage methods for recurrent prostate cancer after failure of primary radiotherapy. *BJU Int* 2010; **105**: 191–201. doi: 10.1111/j.1464-410X.2009.08715.x